Earth Moon Planet (2009) 105:235–247
DOI 10.1007/s11038-009-9333-8

E–ELT: Expected Applications to Asteroid Observations in the Thermal Infrared

Marco Delbó

Received: 27 January 2009 / Accepted: 23 June 2009 / Published online: 18 July 2009

Abstract Applications of the 42m European Extremely Large Telescope (E–ELT) for the physical characterization of asteroids is presented. In particular, this work focuses on the determination of sizes and other physical properties of asteroids from measurements of their heat emission in the thermal infrared (>5 μm). Here we show that E–ELT will be best suited for the physical characterization of some selected asteroids of particular interest, as for instance: (i) targets of sample return missions to near-Earth Asteroids (NEAs); (ii) km and sub-km binary asteroids for which size information will allow their bulk density to be derived; (iii) sizes and values of the thermal inertia of potentially hazardous asteroids (PHAs). These two parameters both affect the Yarkovsky effect, which plays a role in the orbital evolution of km sized asteroids and represents a large source of uncertainty in the Earth impact probability prediction of some PHAs. Thermal inertia is also a sensitive indicator for the presence or absence of thermal insulating regolith on the surface of atmosphere-less bodies. Knowledge of this parameter is thus important for the design and the development of lander- and sample return-missions to asteroids. The E–ELT will also be able to spatially resolve asteroids and detect binaries in a range of sizes that are at present not accessible to present day adaptive optics.

Keywords Asteroids · Thermal infrared · Observations

1 Introduction

Asteroids are the remnants of the planetesimals and the building blocks that formed the inner planets 4.6 billion years ago. Therefore, they conserve the record of the primordial material and possibly the initial conditions existing in the solar nebula at the time of the planet formation process. Information about the nature, chemical composition, sizes, albedos and orbits of the different populations of asteroids is crucial for our understanding

M. Delbó (✉)
UNS, CNRS, Observatoire de la Côte d'Azur, BP 4229 06304, Nice cedex 04, France
e-mail: delbo@oca.eu

of the formation and evolution of the inner planets, including the origin of the organic compounds leading to the development of life on Earth (Morbidelli et al. 2000).

The most fundamental physical property of a minor body is its size. Knowledge of the size allows also the surface reflectivity or geometric albedo (p_V) to be determined (see Sect. 2). We note that the value of p_V is *per se* a very important physical parameter: it is a strong indicator of mineralogical composition of a body: it is well known, for instance, that primitive bodies with carbonaceous composition display low albedos (in general $p_v < 0.1$), whereas objects belonging to more silicaceous (stony) composition have moderate to higher albedos ($0.15 \lesssim p_V \lesssim 0.3$).

The albedo gives also important constraints about the origin of a given body. For example, low or very low value of p_V (e.g. 0.04) can be used to constrain the possible cometary origin of the body.

Knowledge of the size frequency distribution (SFD) and of the distribution of albedos of near-Earth and main belt asteroids, Jupiter Trojans, and Transneptunian bodies severely constrain the models of the formation and early evolution of our Solar System [such as the 'Nice model' (Gomes et al. 2005; Morbidelli et al. 2005; Tsiganis et al. 2005)]. Yet, the SFDs of these population of bodies, are not well known (Bottke et al. 2005; Tedesco et al. 2005; Delbó et al. 2007). Any evidence for differences (or lack thereof) between the SFD of the populations and sub-populations of these bodies will further constrain these models. Furthermore, the SFD of main belt asteroids smaller than about 50 km in diameter is shaped by collisions (Bottke et al. 2005). Knowledge of asteroid sizes is therefore also relevant for studies of the collisional history of these bodies.

In the case of space missions devoted to *in-situ* studies of asteroids, determination of the sizes of the possible targets is essential for mission planning. The albedo is also an indicator for the origin of asteroids and therefore important for the selection of the targets of space missions to NEAs such as the mission Marco Polo. The latter was selected within the program Cosmic Vision of the European Space Agency (ESA) and it is devoted to return back to the Earth a sample of a body of primitive composition.

Furthermore, because the masses of asteroids with satellites can be determined from the orbit of these systems, accurate size determination allows the objects bulk density to be derived. The latter is an important constraint to the body's internal structure and is one of the biggest unknown in the physics of asteroids (Merline et al. 2002).

Moreover, information about the sizes of NEAs and their size distribution is essential for a better understanding of the origin of these bodies: it is, in fact, well established that size dependent non-gravitational forces such as the Yarkovsky effect plays an important role in the delivery of these bodies from the asteroid belt to the near-Earth space (Bottke et al. 2006; Morbidelli et al. 2003). This effect is the change in the orbital elements of small (diameter <10–20 km) asteroids caused by the anisotropic thermal emission of the body's surface, and plays an important role also in the dynamical spreading of asteroid families.

The importance of an accurate knowledge of the sizes of NEAs, and in particular of potentially hazardous asteroids (PHAs), is clear for any evaluation of the impact risk that they pose to our planet and for the development of mitigation strategies. In addition, the orbital evolution of these small asteroids (the large majority of which have effective diameters[1] $D_e \leq 1$ km), is intimately linked to their physical properties: the Yarkovsky effect, which depends on the size, shape, spin vector, and surface thermal characteristics, is the largest source of uncertainty in the Earth impact probability prediction of PHAs, such

[1] For an asteroid with irregular shape we intend the effective diameter: i.e. the diameter of the sphere with the same projected area.

as 1950 DA (Giorgini et al. 2002). This asteroid has a non-negligible probability of impacting the Earth in March 2880. Another very interesting case is represented by the near-Earth object (99942) Apophis. This object will make an extremely close approach to the Earth in 2029, and currently has approximately a one-in-43,000 chance of impacting our planet in 2036.[2] The only size determination available up to now for this object comes from polarimetric observations obtained with the ESO-VLT (Delbó et al. 2007). The strength of the Yarkovsky effect depends also on the temperature distribution on the surface of the body, in particular on the asymmetry between the morning and the evening side (Bottke et al. 2006). The latter is controlled by the spin state of the body and by the thermal inertia of the surface (Brown and Matson 1987; Lagerros 1996; Spencer et al. 1989). Thermal inertia measures the resistance of a material to temperature changes. The thermal inertia of the surface of an asteroid depends on regolith particle size and depth, degree of compaction, and exposure of solid rocks and boulders within the top few centimeters of the subsurface (Mellon et al. 2000). Thermal inertia is also a function of temperature and thus it depends on the heliocentric distance of the body (Keihm 1984; Brown et al. 1987). This temperature dependence should be considered, for instance, when comparison are made between the thermal inertia of main belt asteroids to that of warmer bodies such as near-Earth objects. Knowledge of the thermal inertia of asteroids is thus important because its value can be used to infer the properties of the regolith on the surface. This is especially important for the design of space missions that include lander operations and collection of samples from NEAs.

In the next section we briefly describe how asteroid sizes and other surface properties can be determined from thermal infrared observations. In Sect. 3 the current knowledge of asteroid sizes is briefly reviewed. In the same section on going and future projects devoted to the physical characterization of asteroids, manly of survey-type, are shortly described. In Sect. 5 some possible applications of the E–ELT for the physical characterization of asteroids are discussed.

2 Determination of Asteroid Sizes, Albedos and Thermal Inertia from Infrared Observations

Upon discovery, along with the orbital elements of an asteroid,[3] the only physical information available of a minor body is its absolute visible magnitude[4] H.

The H-value is related to the effective diameter of the body and its geometric visible albedo p_V, via Eq. 1 [see Harris et al. (2002) and references therein].

$$\log p_V = 6.247 - 2\log D_e - 0.4H \tag{1}$$

From Eq. 1 one can derive that

$$\frac{\sigma_{D_e}}{D_e} = 1/2\frac{\sigma_{p_V}}{p_V} \tag{2}$$

[2] JPL Sentry: http://www.neo.jpl.nasa.gov/risk/, January 2009.

[3] Orbital elements, in conjunction with orbital evolution models, allow also to track—to some extent—the past dynamical history of the body.

[4] the magnitude in the *V*–band that would be measured by observing the object at 1 AU distance from both the Sun and the observer, and at zero phase angle. In principle, this parameters is determined—sometime with significant uncertainties—for all known asteroids and can be obtained from e.g. the Minor Planet Center orbital database.

where σ_{D_e} and σ_{p_V} are the uncertainties on the size and albedo, respectively. Because p_V can assume values in the range between 0.03 and 0.6 [see Delbó et al. (2003); Wolters et al. (2002)], Eq. 2 shows that the size can not be reliably estimated from H.

Measurements of asteroids heat emission in the thermal thermal infrared ($\lambda \geq 5$ μm) can be used to derive the sizes of these bodies [see Harris and Lagerros (2002) and references therein] this is because the infrared flux I_{ir} is proportional to D_e^2 and only weakly dependent on the albedo. Once D_e is known, p_V can be determined from Eq. 1. This technique has been used to derive the largest majority of asteroids sizes and albedos.

However, I_{ir} depends also on the temperature distribution on the asteroid surface. So, in order to obtain reliable estimates of asteroid sizes from I_{ir}, the body surface temperature must be estimated or derived from observations. Different models of the surface temperature distribution, the so-called asteroid thermal models, are commonly adopted to calculate the emission of these bodies in the thermal infrared [see Brown (1985); Lebofsky et al. (1986); Spencer et al. (1989); Spencer (1990); Lagerros (1998); Lagerros et al. (1996), (1997), and also (Delbó and Harris 2002; Harris and Lagerros (2002) and references therein]. In the most common situation of bodies for which spin vector and shape information is not available, simplified thermal models based on an assumed spherical shape must be adopted such as the Standard Thermal Model [STM; Lebofsky et al. (1986)], the Near-Earth Asteroid Thermal Model [NEATM; Harris (1998)], and the Fast Rotating thermal Model [FRM; see Harris and Lagerros (2002); Delbó and Harris (2002) and references therein]. The latter work gives all the mathematical formulas needed to implement the above-mentioned thermal models. The parameters of these models are the albedo, the size, and the subsolar temperature (T_{SS}). The latter can be derived from spectroscopic or photometric multi-wavelength observations in the thermal infrared. The model subsolar temperature is adjusted until the calculated thermal infrared emission matches the observed one. In case of photometric measurements in one single band (e.g. the N-band), the temperature can not be constrained from the data, and must be estimated from knowledge of how it varies with the heliocentric distance of the body, the albedo (more reflective surfaces are cooler than darker ones), and the phase angle under which the asteroid is observed. Because $(1 - qp_V)S_{\odot}r^{-2} = \eta\sigma\epsilon T_{SS}^4$, where q is the phase integral, $S_{\odot}$ is the solar constant at 1 AU, r the heliocentric distance, σ the Stephan Boltzmann constant, ε the infrared emissivity, the dependence from the r and p_V is trivial. So, the estimation of the subsolar temperature consist in finding an appropriate value of the so-called beaming parameter η (Lebofsky et al. 1986; Harris 1998). Empirical relations between the value of η and the phase angle under which an asteroid is observed exist: see (Delbó et al. 2003; Wolters et al. 2002).

Sophisticated thermophysical models are nowadays adopted when information about the body's shape and spin vector are known (Emery et al. 1998; Lagerros 1998; Lagerros et al. 1996, 1997; Spencer et al. 1989; Spencer 1990). In the common practice, the parameters of these models that are adjusted to infrared observations are the size of the body, the roughness and the thermal inertia of the surface (Mueller et al. 2007; Delbó and Tanga 2009). We note the accuracy of these models in successfully reproducing diameters, albedos and surface properties of near-Earth and main belt asteroids (Lamy et al. 2008; Mueller et al. 2002, 2004, 2005, 2006). An important aspect of thermophysical modeling is the possibility of including shape models (e.g., from lightcurve inversion techniques; see http://www.astro.troja.mff.cuni.cz/projects/asteroids3D/web.php) to derive more reliable effective sizes and albedos of asteroids.

As demonstrated by Delbó et al. (2007) asteroid sizes can also be derived from polarimetric observations in the visible light. The latter technique allows p_V to be derived from the variation of the degree of the polarization of the light reflected from the surface of the asteroid as function of the phase angle. Once p_V is known, the size can be easily computed from Eq. 1. It is worth to note that the accuracy of size determination from polarimetry is in general poorer than that obtained from radiometry. This is because, in the case of polarimetry, the uncertainty on the H magnitude contributes directly to error on the object size estimation.

Although the sizes and albedos of asteroids are fundamental, these parameters along with other surface thermal properties are known only for a small fraction of the known bodies.

3 Present Knowledge of Asteroid Sizes, Albedos and Thermal Inertia Values

At present, the large majority of asteroid sizes and albedos comes from the Supplemental IRAS Minor Planet Survey [SIMPS Tedesco et al. (2002)], which contains 2228 asteroids, each of them observed at different epochs. Besides some exceptions (e.g. 69 Jupiter Trojan asteroids and some NEAs) these objects are MBAs. However, this catalogue contains only a tiny fraction ($\sim$0.6%) of the currently known population of MBAs, which counts more than 350,000 entries. We also recall the Midcourse Space Experiment (MSX) Infrared Minor Planet Survey that contains diameters and albedos of about 168 asteroids (Tedesco et al. 2002).

A certain number of asteroid sizes and albedos (Shevchenko et al. 2006) is meanwhile coming from occultation observations by amateur astronomers (see http://www.euraster.net/results/index.html). Moreover, the number of predictable asteroid occultations is expected to grow in the future, thanks to the availability of next generation stellar catalogues and asteroid ephemerides (Tanga and Delbó 2007).

Detailed surface thermal properties are known even for less asteroids: for instance thermal inertia has now been determined for about 25 asteroids (Lamy et al. 2008; Delbó and Tanga 2009). Even with this small numbers of bodies, a significant correlation between size and the value of the thermal inertia has been identified (Delbó et al. 2007; Delbó and Tanga 2009). In particular thermal inertia increases with the decreasing size of the body. This is consistent with the fact that smaller asteroids have less thick and mature regolith and more exposed rocks and boulders compared to larger asteroids [see Delbó et al. (2007) and references therein].

An important effort has also been devoted to determine sizes and albedos of NEAs from observations of these bodies in the thermal infrared, radar, and also polarimetry. Up to now, sizes are available for about 90-100 NEAs (see the G. Hahn's data base http://www.earn.dlr.de/nea/table1_new.html).

In the next sections, first of all, we recall some of the most important on going and future surveys devoted to the physical characterization of asteroids, secondly we will investigate the limit of applicability of the E–ELT for the size determination of small and very small asteroids.

4 On Going and Future Projects

The Spitzer Asteroid Catalog (PI D. Trilling) aims at identifying, extracting, cataloging, and analyzing serendipitous observations of asteroids in the Spitzer archive (Trilling et al.

2007). A compilation of at least 35,000 diameters and albedos of asteroids is expected, down to sizes of about 10 km in the main belt.

A complementary program (Exploration Science (ES) proposal, PI D. Trilling; Cycle-6, “The Warm Spitzer NEO Survey: Exploring the history of the inner Solar System and near Earth space”) approved during the warm phase of the Spitzer mission is devoted to the size determination of about 700 NEAs down to $H \sim 20$.

The Akari JAXA/ESA mission (Murakami et al. 2007) just completed its all-sky survey and it is estimated that several thousands asteroids, can be found within the Akari survey.

The Wide-field Infrared Survey Explorer (WISE) is a NASA mission expected to be launched within 2009 (see http://www.wise.ssl.berkeley.edu/index.html). WISE will survey the entire sky in four bands from 3.3 to 23 μm with a sensitivity 1,000 times greater than the IRAS survey. WISE is expected to detect asteroids a million times fainter than (1) Ceres. Because the flux scale with the square of the linear size of the body, WISE should be able to determine the diameter of km-sized bodies in the main belt (Mainzer et al. 2005).

The ESA mission Herschel is well suited for the physical characterization of the colder bodies in our solar system, such as Centaurs and TNOs (Müller et al. 2009). These objects orbiting the sun beyond 10 and 30 AU respectively have surface temperature in general below 100 and 70 K (Delbó 2004). Their thermal emission peaks at wavelengths >20 μm making their observation very challenging from the ground where the atmosphere is opaque at these wavelengths.

Moreover, we recall here that some other smaller surveys devoted to the study of specific classes of objects exists: one of this is the survey of binary asteroids in the thermal infrared carried out with Spitzer by F. Marchis et al (Spitzer Proposal ID #40164). The program aims at better estimating the fundamental properties of binary asteroid systems. Spitzer/IRS spectra (between 5 and 42 μm) have been recorded for 26 selected targets. The data can be used to better refine the sizes, albedos, and eventually bulk-densities of the observed binary systems.

5 Asteroid Observability with the E–ELT in the Thermal Infrared

Although an E–ELT–class telescope will have the sufficient photometric sensitivity to allow sizes of asteroids as small as 1 km in the main belt to be derived, it is clear that such instrument is not appropriate to carry out large surveys. The E–ELT will be better suited to carry out the physical characterization of some peculiar well restricted number of selected targets, whereas the large majority of small bodies size determinations will have to come from infrared surveys, mainly space based.

Two are the most important features of an E–ELT-like telescope for the physical characterization of minor bodies from infrared observations: namely its *high sensitivity*, and its *high spatial resolution*. The first is crucial for the size and albedo determination km and sub-km sized asteroids from photometric observations of their thermal infrared emission.

5.1 Asteroid Size Limits of the E–ELT

In the following, we estimate the limiting size of an asteroid as function of the heliocentric distance, *r*, for which the E–ELT can provide reliable sizes. We require a photometric S/N$\sim$10. This roughly corresponds to a relative error of 10% in the determination of the surface albedo of the body. The latter corresponds to a 5% relative error on the size, assuming that *H* is perfectly known and that the thermal modeling uncertainty is zero. We note that typical thermal models uncertainties are in general $\frac{\sigma_{De}}{D_e} \sim 30\%$ for the STM and $\frac{\sigma_{De}}{D_e} \sim 20\%$ for the NEATM (Harris 2006). In the case of the NEATM $\frac{\sigma_{De}}{D_e}$ can decrease to $\sim 10\%$ if observations are carried out at phase angles <20°, which is often the case for main belt asteroids (Harris 2006). Absolute magnitudes are also known to be affected by significant systematic errors of 0.3 magnitudes or more, mainly for asteroids smaller than ~40–50 km (Parker et al. 2008).

The E–ELT Exposure Time Calculator (ETC)[5] was used to determine the limiting thermal infrared flux measurable with S/R = 10 with one hour of integration in three bands at 5, 10, and 20 μm. These values correspond to the central wavelengths of the M, N, and Q photometric bands respectively where the atmosphere is relatively transparent and narrow band filters are available. These limiting flux values are of about 27, 50, and 100 μJy for a Paranal-like site and of 18, 30, and 50 μJy for a high and dry site (e.g. at 5,000 m). We note also that the expected sensitivities of METIS, the Mid-infrared E–ELT Imager and Spectrograph are expected to be slightly better than the values given above (Brandl et al. 2008).

The limiting flux was then compared with expected fluxes of asteroids as function of *r*. Figure 1 shows the flux density as function of wavelength for bodies at different heliocentric distance (see figure caption for details). Note that for bodies at r >10 AU observations in the thermal infrared from the ground are in general not ideal because the flux densities of these cold objects peaks at wavelengths >20 μm, where our atmosphere transparency is very low.

Figure 2 shows that with the E–ELT asteroids smaller than 100 m can be easily measured up to 2 AU from the Sun. This population includes all NEAs, Mars crosser and Mars Trojans bodies.. In the main belt the E–ELT can be used to measure km and sub-km sized bodies. Current models of the main belt asteroid population expect between 5×10^6 (Bottke et al. 2005) and 10^6 (Tedesco et al. 2005) bodies with sizes larger than 1 km. A large fraction (~15%) of asteroids smaller than 5 km are also expected to be binaries (Pravec and Harris 2007). In the region of Centaurs ($r \sim 10$ AU) the E–ELT can reach objects of 10 km. However, the function of Fig. 2 grows very rapidly as *r* increases, making the physical characterization of Transneptunian objects almost impossible from the Earth.

5.2 Physical Characterization of PHAs with the E–ELT

A possible application of the E–ELT will be the determination the sizes of PHAs, as for instance the NEA (99942) Apophis. Figure 3 shows the expected thermal infrared flux at 10 μm from this asteroid as function of time between the years 2009 and 2030. The flux was calculated using the NEATM and assuming the present best estimates of the size and the albedo (Delbó et al. 2007) for this asteroids and a ground based observer. Note that Apophis' 10 μm flux is in general below 1 mJy, making difficult, if not impossible, the physical characterization of this body with present day thermal infrared facilities installed

[5] The E–ELT Exposure Time Calculator can be found at http://www.eso.org/observing/etc/bin/gen/form?VIEW.APPLIC.HTM=ins-elt.htm+VIEW.APPLIC.DIC.HTM=ins-elt-dic.html for imaging and at http://www.eso.org/observing/etc/bin/gen/form?INS.NAME=E-\elt+INS.MODE=spectro for spectroscopy. For this work, the Version 2.13 was used for imaging and the version Version 2.12 for the spectroscopic mode (January 2009).

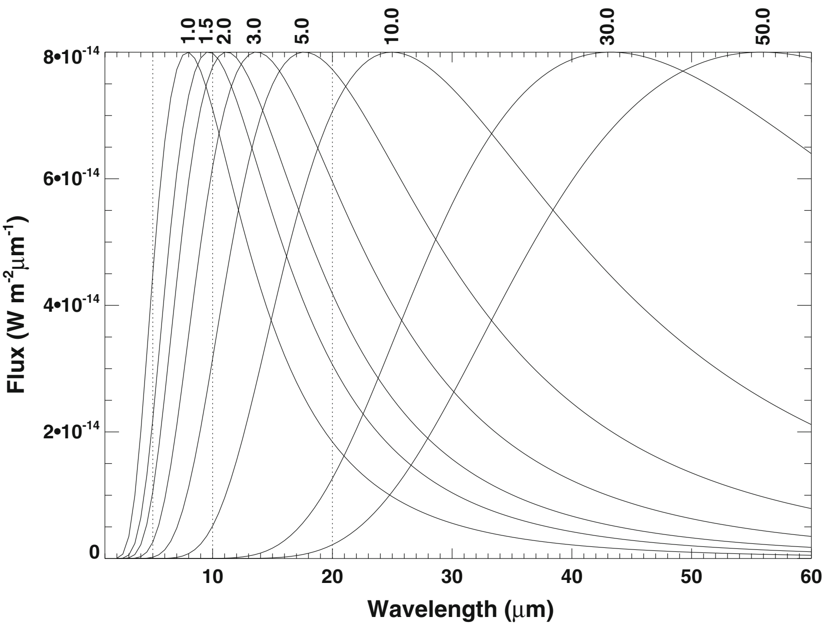

Fig. 1 Thermal infrared flux as function of wavelength emitted by atmosphere-less bodies at different heliocentric distances, r. The latter is indicated by the values in AUs on top of the plot. The geocentric distance is $\Delta = r - 1$ AU and the phase angle equal to 0° For all bodies $p_V = 0.2$, $\varepsilon = 0.9$. The sizes of the bodies are chosen such that the flux density at peak wavelength is equal to 8.0×10^{-14} $W\,m^{-2}$ μm^{-1}. The resulting diameters are reported in Table 1. Fluxes are given in $W\,m^{-2}$ μm^{-1} and can be easly converted into Jansky using the following formula: $f(\lambda)_{Jy} = f(\lambda)_W * \lambda^2 * 3.3357 \times 10^{11}$, where $f(\lambda)_{Jy}$ is the monochromatic flux density in Jy at the wavelength λ (in μm) and $f(\lambda)_W$ is the flux in units of $W\,m^{-2}$ μm^{-1}. The flux depends also on the surface thermal inertia and macroscopic roughness, the body's rotation period and pole obliquity. In general these parameters are poorly known for the large majority of minor bodies. However, their overall effects on the infrared flux can be taken into account by varying the value of the beaming parameter η in the NEATM. Here we assume a conservative value $\eta = 2$. This makes a rather cool surface temperature distribution resulting in a lower flux with respect to surfaces in instantaneous thermal equilibrium with sunlight with $\eta = 1$. The flux can be scaled to any value of the body's size and Δ taking into account that $I_{ir} \propto D_e^2\ \Delta^{-2}$. Three vertical dotted lines are drawn at 5, 10, and 20 μm roughly corresponding to the central wavelengths of the M, N, and Q photometric bands respectively

on ground based telescopes, such as VISIR at the 8m VLT telescope. This instrument has a 10 μm limiting flux of about 8 mJy, 10σ/1h. With today ground based instruments, (99942) Apophis can only be observed during the Earth very close approaches that this body undergoes in 2013, 2021, and 2029. Note that during the close approaches the phase angle of the body varies rapidly and it is in general large (e.g. >45°): diameters derived from simple thermal models (such as the NEATM) are less reliable when observations are carried out at large phase angle (Harris 2006). On the other hand, the E–ELT sensitivity in the thermal infrared is such that (99942) Apophis observations can be carried out at any time.

5.3 The Advantage of the High Spatial Resolution of the E–ELT

Another crucial feature of the E–ELT is its spatial resolution (see Table 2), which can be used to directly resolve km and sub-km sized NEA during their close Earth approaches.

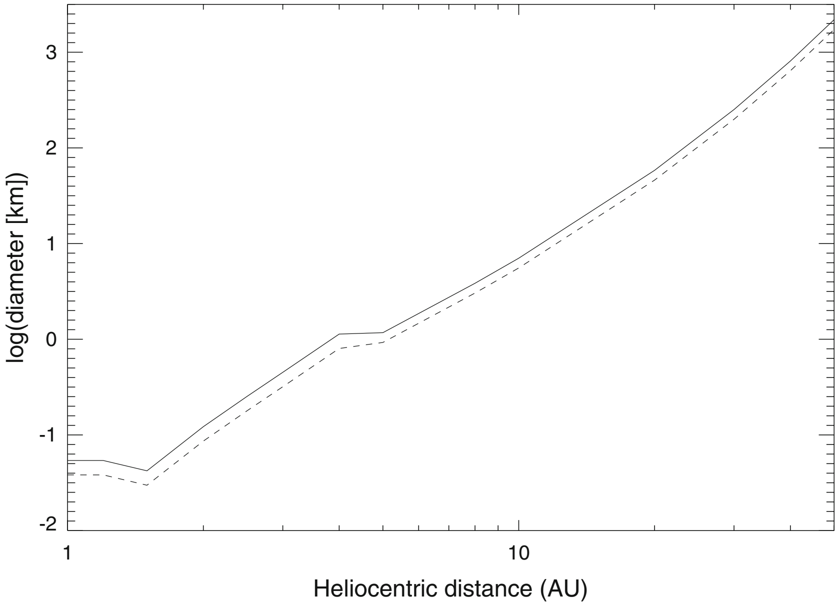

Fig. 2 Limiting size of a minor body for which the E–ELT can provide physical characterization as function of the heliocentric distance. The limiting size corresponds to the value of D_e of an asteroid for which the 10 μm flux is equal to the lowest observable flux with the E–ELT (10σ/1h; see text for details). If the asteroid has an $r > 4$ AU the 20 μm flux is used instead. The distance to the observer, Δ, is $r-1$ and $\alpha = 0°$ if $r > 1.5$ AU, $\Delta = 0.5$ AU and $\alpha = 45°$ otherwise. The continuous line corresponds to observations carried out from a Paranal-like site, the dashed line to a drier and higher (5,000 m) site (see the E–ELT–ETC for further details)

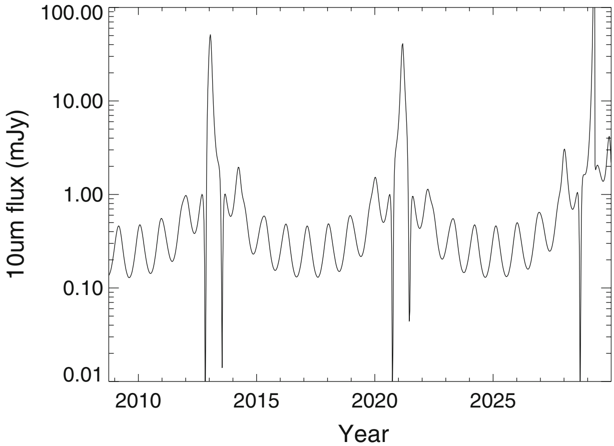

Fig. 3 Expected thermal infrared flux of the NEA (99942) Apophis between January 1, 2010 and April 13, 20036 date of the possible Earth impact. The flux was calculated assuming $D_e = 270$ m, $p_V = 0.33$, using the NEATM (Harris 1998)

Likewise, multi 10 km-sized asteroids in the main belt can easily be resolved. There are about 100 asteroids larger than 100 km (Bottke et al. 2005). The E–ELT will be, in principle, capable of putting between 10 and 20 pixels across these objects in

Table 1 Thermal infrared fluxes of asteroids with different diameters at different heliocentric distances. Sizes are chosen such that their infrared fluxes at the peak wavelength are all equal to 8×10^{-14} W m^{-2} μm^{-1}: see Fig. 2

r (AU)	D_e (km)	I_5 (Jy)	I_{10} (Jy)	I_{20} (Jy)	λ_{peak}
1.0	10.182	1.069e-01	2.185e-01	3.754e-01	8.0
1.5	16.904	3.435e-02	8.851e-02	1.832e-01	9.5
2.0	24.217	1.162e-02	3.638e-02	8.802e-02	11.0
3.0	40.199	1.580e-03	6.848e-03	2.151e-02	13.5
5.0	76.117	4.937e-05	3.578e-04	1.697e-03	17.5
10.0	181.021	4.880e-08	9.059e-07	9.126e-06	25.0
30.0	714.737	3.749e-16	7.235e-14	4.751e-12	43.0
50.0	1353.464	5.726e-22	5.522e-19	1.314e-16	56.0

Table 2 E–ELT spatial resolution at different wavelengths in the infrared

λ (µm)	ρ (mas)	km at 0.1 AU	km at 1.5 AU
1.0	5	0.4	5.4
2.5	12	0.9	12.9
3.0	15	1.1	16.2
5.0	24	1.7	25.9
10.0	50	3.5	52.9
20.0	100	7.0	105.8

adaptive-optics images taken in the near-infrared. The number of asteroids increases to about 200 if we consider all asteroids larger than 50 km (Bottke et al. 2005). Sizes of asteroids from adaptive-optics imaging can be used to test the reliability of the thermal models described above (Cellino et al. 2003; Ragazzoni et al. 2000).

Another fascinating field in which adaptive optics observations at the E–ELT can give a fundamental contribution is in the characterization of binary asteroids. In the last few years, several asteroids consisting of two very close components, or having small satellites, have been discovered. Their observation is extremely important, since information on the revolution period and separation allows the direct determination of the total mass of the system. A size estimate, when available, allows the density of the body to be derived, thus providing a direct insight of the internal structure of the asteroid.

The prospects of future discoveries of binary asteroids with E–ELT–class telescopes are described elsewhere (Walsh et al. 2009). Here we would like to point out that with the angular resolution of the E–ELT most of the known binary asteroids can have their components separated allowing a physical characterization of the primary and the secondary separately. This would be important to constrain the physical mechanisms responsible for the formation of satellites. Some of these processes are thought to produce a differentiation in the surface properties of the primary with respect to those of the satellites (Delbó et al. 2008; Walsh et al. 2008) observable by means of near infrared spectroscopy and/or thermal infrared measurements. In the case of NEAs, at $r \sim 1$ AU, surface temperatures are warm enough that significant thermal flux is emitted at 5 µm. The E–ELT 5 µm resolution allows several binary NEAs to be separated at this wavelength. If the sizes of the bodies are known (e.g. from 10 µm *radiometry*), the flux 5 µm flux from the different component of the system can be translated into brightness temperatures. Asteroid surface temperatures are function of the thermal inertia. This latter parameter, which is related to the regolith depth and compaction and/or exposure of bare rocks on the surface, can then be constrained separately for the primaries and the secondaries of binary systems.

Note that 5 μm resolution of the E–ELT is sufficient to put some pixel across multi-km sized NEAs during Earth close approaches. Taking into account also of the relative rapid rotation of these bodies [periods are in general between 2.5 and 10 h (Warner et al. 2009)], surface temperature maps can be generated from 5 μm images. An interesting application of this is a careful estimation of the Yarkovsky effect. The Yarkovsky effect is strongly affected by the way temperatures are distributed on the surface of asteroids, however, at present, very little is known about the properties of the thermal emission of asteroids in the km size range.

6 Conclusions

Future extremely large telescopes such as the E–ELT equipped with state of the art medium infrared camera provide a powerful tool to perform size determination of km sized asteroids in the main belt and sub-km sized bodies in the near-Earth space.

Most of the known binary asteroid will be separated in the thermal infrared, allowing the temperature of the two components to be separately measured.

The E–ELT spatial resolution will allow asteroid thermal maps to be constructed. This is important for the evaluation of the Yarkovsky effect and also to study in details the surface makeups of these bodies.

The above-mentioned applications and the exploitation of the full potential of E–ELT medium infrared observations will require adequately powerful thermal models such as the thermophysical models.

Acknowledgements This work was partially carried out while Marco Delbó was a Henri Poincaré Fellow at the Observatoire de la Côte d'Azur. The Henri Poincaré Fellowship is funded by the CNRS-INSU, the Conseil Général des Alpes-Maritimes and the Rotxary International – District 1730. The author wishes to thank the organizers of the workshop "Future Ground based Solar System Research: Synergies with Space Probes and Space Telescope" hold in the beautiful Elba island, Italy, in September 2008. In particular, the kind invitation from Gian Paolo Tozzi and Ulli Kaufl in acknowledge. Part of this paper was written in the library of the British Museum (London, UK). The comments and the suggestions of an anonymous referee are gratefully acknowledged.

References

W.F. Bottke, D.D. Durda, D. Nesvorný, R. Jedicke, A. Morbidelli, D. Vokrouhlický, H. Levison, The fossilized size distribution of the main asteroid belt. Icarus **175**, 111 (2005)

W.F. Bottke, D.D. Durda, D. Nesvorný, R. Jedicke, A. Morbidelli, D. Vokrouhlický, H.F. Levison, Linking the collisional history of the main asteroid belt to its dynamical excitation and depletion. Icarus **179**, 63 (2005)

W.F. Bottke, D. Vokrouhlický, D.P. Rubincam, D. Nesvorný, The yarkovsky and yorp effects: Implications for asteroid dynamics. Annu. Rev. Earth. Planet. Sci. **34**, 157 (2006)

B.R. Brandl, R. Lenzen, E. Pantin, A. Glasse, J. Blommaert, L. Venema, F. Molster, R. Siebenmorgen, H. Boehnhardt, E. van Dishoeck, P. van der Werf, T. Henning, W. Brandner, P-O. Lagage, T.J.T. Moore, M. Baes, C. Waelkens, C. Wright, H.U. Käufl, S. Kendrew, R. Stuik, L. Jolissaint, in *METIS: The Mid-Infrared E-ELT Imager and Spectrograph. Ground-Based and Airborne Instrumentation for Astronomy II*, vol. 7014, ed. by McLean (2008), p. 55

R.H. Brown, Ellipsoidal geometry in asteroid thermal models—the standard radiometric model. Icarus **64**, 53 (1985). ISSN 0019-1035

R.H. Brown, D.L. Matson, Thermal effects of insolation propagation into the regoliths of airless bodies. Icarus **72**, 84 (1987). ISSN 0019-1035

A. Cellino, E. Diolaiti, R. Ragazzoni, D. Hestroffer, P. Tanga, A. Ghedina, Speckle interferometry observations of asteroids at tng*. Icarus **162**, 278 (2003)

M. Delbó, The nature of near-Earth asteroids from the study of their thermal infrared emission. Ph.D. thesis (2004)

M. Delbó, A. Cellino, E.F. Tedesco, Albedo and size determination of potentially hazardous asteroids: (99942) apophis. Icarus **188**, 266 (2007)

M. Delbó, A. Dell'Oro, A.W. Harris, S. Mottola, M. Mueller, Thermal inertia of near-Earth asteroids and implications for the magnitude of the Yarkovsky effect. Icarus **190**, 236 (2007)

M. Delbó, A.W. Harris, R.P. Binzel, P. Pravec, J.K. Davies, Keck observations of near-Earth asteroids in the thermal infrared. Icarus **166**, 116 (2003)

M. Delbó, A.W. Harris, Physical properties of near-earth asteroids from thermal infrared observations and thermal modeling. Meteorit. Planet. Sci. **37**, 1929 (2002)

M. Delbó, P. Tanga, Thermal inertia of main belt asteroids smaller than 100 km from iras data. Planet. Space Sci. **57**(2), 259–265 (2009)

M. Delbó, K. Walsh, M. Mueller, The cool surfaces of binaries near-Earth asteroids. American Astronomical Society, DPS meeting #40, #25.08. Bull. Am. Astron. Soc. **40**, 433 (2008)

J.P. Emery, A.L. Sprague, F.C. Witteborn, J.E. Colwell, R.W.H. Kozlowski, D.H. Wooden, Mercury: thermal modeling and mid-infrared (5–12 m) observations. Icarus **136**, 104 (1998)

J.D. Giorgini, S.J. Ostro, L.A.M. Benner, P.W. Chodas, S.R. Chesley, R.S. Hudson, M.C. Nolan, A.R. Klemola, E.M. Standish, R.F. Jurgens, R. Rose, A.B. Chamberlin, D.K. Yeomans, J.L. Margot, Asteroid 1950 da's encounter with earth in 2880: physical limits of collision probability prediction. Science **296**, 132 (2002)

R. Gomes, H.F. Levison, K. Tsiganis, A. Morbidelli, Origin of the cataclysmic late heavy bombardment period of the terrestrial planets. Nature **435**, 466 (2005)

A.W. Harris, A thermal model for near-earth asteroids. Icarus **131**, 291 (1998)

A.W. Harris, The surface properties of small asteroids from thermal-infrared observations. Asteroids **229**, 449 (2006)

A.W. Harris, J.S.V. Lagerros, in *Asteroids in the Thermal Infrared*, ed. by W.F. Bottke Jr., A. Cellino, P. Paolicchi, R.P. Binzel. Asteroids III (University of Arizona Press, Tucson, 2002), pp. 205–218

S. J. Keihm, Interpretation of the lunar microwave brightness temperature spectrum—feasibility of orbital heat flow mapping. Icarus **60**, 568 (1984). ISSN 0019-1035

J.S.V. Lagerros, Thermal physics of asteroids. i. effects of shape, heat conduction and beaming. A&A **310**, 1011 (1996)

J.S.V. Lagerros, Thermal physics of asteroids. iii. irregular shapes and albedo variegations. A&A **325**, 1226 (1997)

J.S.V. Lagerros, Thermal physics of asteroids. iv. thermal infrared beaming. A&A **332**, 1123 (1998)

P.L. Lamy, L. Jorda, S. Fornasier, O. Groussin, M.A. Barucci, J. Carvano, E. Dotto, M. Fulchignoni, I. Toth, Asteroid 2867 steins. iii. spitzer space telescope observations, size determination, and thermal properties. A&A **487**, 1187 (2008)

L.A. Lebofsky, M.V. Sykes , E.F. Tedesco, G.J. Veeder, D.L. Matson, R.H. Brown, J.C. Gradie, M.A. Feierberg, R.J. Rudy, A refined 'standard' thermal model for asteroids based on observations of 1 ceres and 2 pallas. Icarus **68**, 239 (1986). ISSN 0019-1035

A.K. Mainzer, P. Eisenhardt, E.L. Wright, F.C. Liu, W. Irace, I. Heinrichsen, R. Cutri, V. Duval, in *Preliminary Design of the Wide-Field Infrared Survey Explorer (WISE). UV/Optical/IR Space Telescopes: Innovative Technologies and Concepts II*, vol. 5899, ed. by H.A. MacEwen. Proceedings of the SPIE, (2005), pp. 262–273

M.T. Mellon, B.M. Jakosky, H.H. Kieffer, P.R. Christensen, High-resolution thermal inertia mapping from the mars global surveyor thermal emission spectrometer. Icarus **148**, 437 (2000)

W.J. Merline, S.J. Weidenschilling, D.D. Durda, J.L. Margot, P. Pravec, A.D. Storrs, in *Asteroids do have Satellites*, ed. by W.F. Bottke Jr., A. Cellino, P. Paolicchi, R.P. Binzel. Asteroids III (University of Arizona Press, Tucson, 2002), pp. 289–312

A. Morbidelli, J. Chambers, J.I. Lunine, J.M. Petit, F. Robert, G.B. Valsecchi, K.E. Cyr, Source regions and time scales for the delivery of water to earth. Meteorit. Planet. Sci. **35**, 1309 (2000)

A. Morbidelli, H.F. Levison, K. Tsiganis, R. Gomes, Chaotic capture of jupiter's trojan asteroids in the early solar system. Nature **435**, 462 (2005)

A. Morbidelli, D. Vokrouhlický, The yarkovsky-driven origin of near-earth asteroids. Icarus **163**, 120 (2003)

M. Mueller, Surface properties of asteroids from mid-infrared observations and thermophysical modeling. Ph.D. Thesis (2007)

M. Mueller, A.W. Harris, S.J. Bus, J.L. Hora, M. Kassis, J.D. Adams, The size and albedo of rosetta fly-by target 21 lutetia from new irtf measurements and thermal modeling. A&A **447**, 1153 (2006)

T.G. Müller, Herschel Open Time Key Programme; TNOs are cool: a survey of the transneptunian region. Earth Moon Planets, this issue (2009)

T.G. Müller, J.S.V. Lagerros, Asteroids as calibration standards in the thermal infrared for space observatories. A&A **381**, 324 (2002)

T.G. Müller, T. Sekiguchi, M. Kaasalainen, M. Abe, S. Hasegawa, Thermal infrared observations of the hayabusa spacecraft target asteroid 25143 itokawa. A&A **443**, 347 (2005)

T.G. Müller, M.F. Sterzik, O. Schütz, P. Pravec, R. Siebenmorgen, Thermal infrared observations of near-earth asteroid 2002 ny40. A&A **424**, 1075 (2004)

H. Murakami and 92 colleagues, The Infrared Astronomical Mission AKARI. Publ. Astron. Soc. Jpn. **59**, 369 (2007)

A. Parker, Ž. Ivezić, M. Jurić, R. Lupton, M.D. Sekora, A. Kowalski, The size distributions of asteroid families in the sdss moving object catalog 4. Icarus **198**, 138 (2008)

P. Pravec, A.W. Harris, Binary asteroid population. 1. angular momentum content. Icarus **190**, 250 (2007)

R. Ragazzoni, A. Baruffolo, E. Marchetti, A. Ghedina, J. Farinato, T. Niero, Speckle interferometry measurements of the asteroids 10-hygiea and 15-eunomia. A&A **354**, 315 (2000)

V.G. Shevchenko, E.F. Tedesco, Asteroid albedos deduced from stellar occultations. Icarus **184**, 211 (2006)

J.R. Spencer, A rough-surface thermophysical model for airless planets. Icarus **83**, 27 (1990). ISSN 0019-1035

J.R. Spencer, L.A. Lebofsky, M.V. Sykes, Systematic biases in radiometric diameter determinations. Icarus **78**, 337 (1989). ISSN 0019-1035

P. Tanga, M. Delbó, Asteroid occultations today and tomorrow: toward the gaia era. A&A **474**, 1015 (2007)

E.F. Tedesco, A. Cellino, V. Zappalá, The statistical asteroid model. i. the main-belt population for diameters greater than 1 km. Astron. J. **129**, 2869 (2005)

E.F. Tedesco, M.P. Egan, S.D. Price, The midcourse space experiment infrared minor planet survey. Astron. J. **124**, 583 (2002)

E.F. Tedesco, P.V. Noah, M. Noah, S.D. Price, The supplemental iras minor planet survey. Astron. J. **123**, 1056 (2002)

D.E. Trilling, B. Bhattacharya, M. Blaylock, J.A. Stansberry, M.V. Sykes, L.H. Wasserman, The spitzer asteroid catalog: albedos and diameters of 35,000 asteroids. American Astronomical Society, DPS meeting #39, #35.15. Bull. Am. Astron. Soc. **39** 484 (2007)

K. Tsiganis, R. Gomes, A. Morbidelli, H.F. Levison, Origin of the orbital architecture of the giant planets of the solar system. Nature **435**, 459 (2005)

K.J. Walsh, The future of binary asteroid detection. Earth Moon Planets, this issue (2009)

K.J. Walsh, D.C. Richardson, P. Michel, Rotational breakup as the origin of small binary asteroids. Nature **454**, 188–191 (2008)

B.D. Warner, A.W. Harris, P. Pravec, The asteroid lightcurve database. Icarus **202**, 134–146 (2009)

S.D. Wolters, S.F. Green, N. McBride, J.K. Davies, Optical and thermal infrared observations of six near-Earth asteroids in 2002. Icarus **175**, 92–110